INTERNATIONAL JOURNAL OF AGRICULTURE & BIOLOGY
ISSN Print: 1560–8530; ISSN Online: 1814–9596
22–0258/2022/28–6–341–351
DOI: 10.17957/IJAB/15.1987
http://www.fspublishers.org

Full Length Article

Biosynthesis of *Chaetomium globosum*-made ZnO@Ag@Chitosan Nanoparticles and their Potential as an Eco-Friendly Bio-Fungicide against Fungal Root Diseases of Cucumber and Tomato

Wafaa Haggag[1*] and May Eid[2]
[1]*Department of Plant Pathology, Agricultural and Biological Research Institute, National Research Centre, Cairo, Dokki, Egypt*
[2]*Department of Spectroscopy Department, Physics Institute, National Research Centre, Cairo, Dokki, Egypt*
[*]For correspondence: wafaa_haggag@yahoo.com
Received 17 June 2022; Accepted 16 August 2022; Published 12 December 2022

Abstract

In vitro and *in vivo* studies were conducted to investigate the biosynthesis of ZnO@Ag@Chitosan nanoparticles (NPs) from *Chaetomium globosum* as an eco-friendly biofungicide against fungal root rot diseases of cucumber and tomato caused by *Rhizoctonia solani, Sclerotinia sclerotiorum, Fusarium oxysporum, F. solani*, *Macrophomina phaseolina, Phytophthora parasitica, Pythium ultimum, Alternaria alternata* and *Colletotrichum gloeosporioides*. The physico-chemical characterization using UV–visible spectroscopy, FTIR and HRTEM proved the formation ZnO@Ag@Chitosan NPs. The distinct absorbance peak was discovered at 430 nm. Using Fourier transform infrared (ATR-FTIR) spectroscopy, the extent vibrations of chitosan at 3431 cm^{-1}. In comparison to the crude metabolites of *C. globosum*, ZnO@Ag@Chitosan nanoparticles from *C. globosum* inhibited the fungal growth of all tested pathogens at low concentrations. All antioxidant activities of ZnO@Ag@Chitosan, *i.e.*, reducing power, scavenging of DPPH [1,1-Diphenyl-2-picrylhydrazyl] radical, scavenging of nitric oxide and ABTS free radical scavenging activities were increased. The hematological alanine aminotransferase, serum aspartate aminotransferase, and creatinine concentrations of white albino ZnO@Ag@Chitosan NPs were investigated, showing that the NPs were extremely safe. In the greenhouse, ZnO@Ag@Chitosan nanoparticles reduced the incidence of root diseases in tomato and cucumber roots after treating them with 500 mg L^{-1} suspension of ZnO@Ag@Chitosan NPs and increased crop yield. At the same time, higher levels of peroxidase, polyphenoloxidase and chitinase were detected. In addition, photosynthetic pigments such as chlorophyll a and b and carotenoids were also increased. This study concludes that nanoparticle ZnO@Ag@Chitosan synthesized from *C. globosum* metabolite is effective as an eco-friendly biofungicide against soil-borne fungal pathogens. © 2022 Friends Science Publishers

Keywords: Antioxidant activities; Biofungicides; *Chaetomium globosum*; Chitosan; Cucumber; Nanoparticles; Root diseases; Tomato

Introduction

In Egypt and many other nations around the world, major soil and seeds borne plant pathogens such as *Fusarium oxysporum, F. solani, Sclerotinia sclerotiorum, Phytopthora parasitica, Pythium ultimum, Rhizoctonia solani, Colletotrichum gloeosporioides* (El-Kaed *et al.* 2021), *Macrophomina phaseolina* (Javed *et al*. 2021), *Alternaria alternata* (Javaid and Samad 2012) and Sclerotium rolfsii (Javaid and Khan 2016) cause various deadly and destructive diseases.

Plant diseases are being controlled by beneficial microorganisms like plant growth promoting rhizobacteria (PGPR), *Trhichoderma* spp. and *Penicillium* spp. as a secure strategy for agricultural and environmental sustainability (Haggag *et al.* 2015; Sharf *et al*. 2021; Khan and Javaid 2020, 2022). *C. globosum* can control *Fusarium* species, *Phytophthora* species, *C. gloeosporioides*, and other plant diseases (Moya *et al*. 2016). Compared to commercial agrochemicals, agriculture uses of nanotechnology are expanding across a variety of fields, including nutrition, pathogen detection and disease control (Haggag *et al.* 2018). Nanomaterials are used to create biofungicides, which have been shown to have antibacterial, antifungal, and antiviral properties against phytopathogenic microbes *in vitro*, in a greenhouse, and in the field (Farhat *et al*. 2018; Haggag *et al*. 2018; Um-e-Aiman *et al.* 2021). Scientists are interested in surface plasmon (SP), which is produced when a metal nanostructure and a dielectric interact. Among its many uses are plasmon lasers and

enhancing the light absorption and Raman scattering intensity of materials close to its surface (Okamoto *et al.* 2019a). Recent significant advancements in the luminescence intensity and efficiency of light-emitting materials and systems have made SP-mediated emission a popular research topic. By capping the Ag layer, Okamoto *et al.* (2019b) showed a significant PL enhancement of InGaN/GaN quantum wells, demonstrating the significance of SPs-mediated emission in raising LED efficiency (Lu *et al.* 2011). Zinc oxide nanoparticle production methods have been described by a number of organizations. These methods include hydrothermal synthesis, alkali precipitation, thermal breakdown, organo-zinc hydrolysis and more. In a 120°C autoclave, Yang *et al.* (2002) used a CTAB-aided hydro-thermal ZnO nano-wire. ZnO nanorods and prisms were produced by Wang *et al.* (2006) using zinc foil, NaOH and CTAB at a temperature of 160°C. According to Fageria *et al.* (2014), gold nanoparticles on the surface of ZnO can be used to achieve photocatalysis. Zheng *et al.* (2007) used a solvothermal method to create Ag/ZnO heterostructures with variable silver content for use in photocatalysis. Zhou *et al.* (2011) conducted research on ZnO's morphology and application in photocatalysis. The polymer-based methodology is one of the many synthetic techniques used to create metallic nanoparticles, and it has garnered a lot of interest. There are several simple processes for creating silver nanoparticles that use chitosan as a mediator (Hajji *et al.* 2019; Haggag and Eid 2022). A polycationic amino polysaccharide, chitosan (CS) is derived from the chitin present in fungi and crustacean shells. Due to the appealing properties brought on by the presence of functional groups (amino and hydroxyl), this biocompatible and biodegradable polymer has a wide range of applications in biology (Eid *et al.* 2019; Kutawa *et al.* 2021). In this study, ZnO@Ag@Chitosan nanoparticles were biosynthesized from an active metabolite of *C. globosum*, and their antifungal, antioxidant, and biosafety activities were assessed. Additionally, their potential as an environmentally friendly biofungicide to lessen diseases brought on by soil-borne pathogens of tomato and cucumber in greenhouse conditions was assessed.

Materials and Methods

Soil-borne fungal pathogens *i.e., F. oxysporum, F. solani, S. sclerotiorum, R. solani, M. phaseolena, P. parasitica, P. ultimum, A. alternata* and *C. gloeosporioides* were isolated from tomato and cucumber diseased plants grown in greenhouses in Boheria Governorate, Egypt and identified in department of Plant Pathology, National Research Centre, Egypt. We used *Chaetomium globosum,* which had previously been isolated from healthy tomato plants and identified in the Plant Pathology Department of the National Research Centre. For 10 days, fungal cultures were grown in potato dextrose agar (PDA) plates at 25°C. The culture was identified according to Arx *et al.* (1986).

Green synthesis of Ag@cs by *C. globosum*

For 7 days, C. *globosum* was grown on potato dextrose medium at 28°C and pH 7. The broth medium was filtered with filter paper and a 100 mL solution (79 mL filtrate plus 21 mL distilled water) was mixed at room temperature with Silver Nitrate (0.1) and adjusted to pH 9 with 1 N HCl and 10 *M* NaOH. The silver formation was detected using UV-vis absorption analysis at 400 nm (Osman *et al.* 2016).

Zinc oxide preparation

At 60°C, 5 g of zinc acetate were dissolved in 100 mL of distilled water. In a separate pot, 4 g NaOH was dissolved in 100 mL distilled water and dropped onto the zinc acetate solution dropwise. Then, the pellet was washed with filtrated and distilled water, dried at 60°C for 24 h, calcined at 400°C for 4 h and centrifugation at 10000 rpm at 10°C for 20 min (Zhang *et al.* 2009).

Preparation of Ag@zno@cs (core/shell)

Ag@CS (2 g) was mixed with zinc oxide (2 g), ground for 15 min to get a fine powder, dispersed in distilled water, then centrifuged at 10000 rpm for 20 min at 10°C and the pellet was dried at 50°C for 24 h (Vijayakumar *et al*. 2013).

Characterization of ZnO NPs, Ag@CS NPs, Ag@ZnO@CS NPs

A UV–vis spectrophotometer (JASCO, V-530) with a 400 nm resolution was used. ATR-FTIR spectra were measured using a Perkin Elmer FTIR spectrophotometer equipped with a TGS detector and 2 mg of each sample to depict the functional groups responsible for metallic ion reduction. The spectra were captured at a resolution of 4.0 cm^{-1} and 64 scans were combined to achieve a reasonable signal-to-noise ratio. The dried extract powders were tested in parallel. The crystalline structure of the developed phases was examined. The Cu K radiation (1.5418) and a scanning speed of 0.3 S were used on the Bruker XRD X-ray powder diffractometer. The operating voltage and current were both set to 40 kV and 40 mA.

The zeta potential of core-shell nanoparticles was measured using a Zetasizer 1000 at 633 nm at a fixed refractive index of the respective formulation to assess their stability. At pH 7.0, the size of Ag@ZnO@CS nanoparticles (NPs) was measured using a particle size analyzer (PSA: Malvern Zeta Sizer Nano ZS).

***In vitro* bioassay test**

Agar well diffusion assay: The antifungal activity of ZnO@Ag@Chitosan NPs using agar well diffusion assay at concentrations of 50, 250 and 500 mg L^{-1} were tested against fungal growth of *F. solani, F. oxysporum, R. solani,*

M. phaseolena, *S. sclerotiorum*, *P. parasitica*, *P. ultimum*, *A. alternata* and *C. gloeosporioides* (Hongtao *et al*. 2013).

Crude metabolite of *Chaetomium* was prepared by grown on PDB medium for 21 days at room temperature (25–30°C). Biomass was filtrate, dried at room temperature for 7 days and crushed into fine powder using grinder. Metabolite was extracted using successive solvents of ethyl acetate (1:1 v/v) and methanol (1:1 v/v) (Bhardwaj *et al*. 2015). Solvent was evaporated and the residues compound was dried in rotator vacuum evaporator to harvest the crude metabolite.

Crude extract metabolite of *C. globosum* was tested against pathogens using concentrations of 0, 50, 250 and 500 mg L^{-1}. Crude metabolite was dissolved in dimethyl sulfoxide (2%). Colony diameter (mm) was measured after five days using five replicates for each treatment. As a control, carbendazim 50% wettable powder (WP) was used at recommended dose.

Antioxidant assay

Reducing power: The percentage inhibition was determined using an Oyaizu (1986). The Ag@ZnO@CS NPs and metabolite (0.2–1.0 mg mL^{-1}) were mixed with 2.5 mL of water and methanol, 2.5 mL of sodium phosphate buffer (200 m*M*; pH 6.6) and 1% potassium ferricynide (2.5 mL) and incubated for 20 min at 50°C. Following that, 2.5 mL of 10% trichloroacetic acid was added and centrifuged at 200 g for 10 min. The upper layer (2.5 mL) was mixed with deionized water and 0.5 mL of 0.1% ferric chloride. A spectrophotometer set to 700 nm was used to measure absorbance against a blank. Assay for diphenyl-scavenging activity of 1,1-diphenyl-2-picrylhydrazyl (DPPH). Hu *et al*. (2014) described a method for measuring the activity of produced Diphenyl 1 picrylhydrazyl (DPPH) *via* ZnO@Ag@Chitosan NPs. The sample solution (10 mg mL^{-1}) was combined with DPPH in ethanol (180 mol L^{-1}) and incubated with water at 25°C for 30 min. The absorbance was evaluated with a UV–visible spectrometer at 517 nm, with three duplicates for each sample (the control was distilled water instead of DPPH). The scavenging effect was calculated by the following equation: DPPH+ scavenging activity (%) = [(Abs Control – Abs Sample)]/(Abs Control)]x100 where Abs Control was the absorbance of DPPH+ + methanol; Abs Sample is the absorbance of DPPH+ + sample extract /standard.

Scavenging activity for nitric oxide: The ability of nitric oxide to scavenge free radicals was investigated (Marcocci *et al*. 1994). 5.0 mL of reaction mixture including or not containing ZnO@Ag@Chitosan NPs and crude metabolite was combined with sodium nitroprusside (SNP) (5 m*M*), phosphate buffered saline at pH 7.3 and incubated at 25°C for 180 min. Three replicates were used to test nitric oxide scavenging at 540 nm using conventional sodium nitrite salt solutions.

Free radical scavenging activity (ABTS•+) assay: The ABTS free radical scavenging assay was performed using the Zhishen *et al*. (1999) method. The reaction mixture of 2.5 m*M* ABTS (2,2'-azino-bis [3-ethylbenzthiazoline-6-sulfonic acid] diammonium salt) and 1.0 m*M* AAPH (2,2'-azobis-[2-amidinopropane] HCl) in 100 mL phosphate-buffered saline solution (100 m*M* potassium phosphate buffer at pH 7.4 containing 150 m*M* (Whatman Inc., Florham Park, NJ). At 734 nm and 37°C, the absorbance was measured using a microplate reader.

Biosafety and toxicity studies

Tested animals: Female albino rats Rattus norvegicus var. albinos (weighing 110–120 g) were employed in this experiment. The rats were kept at a constant temperature of 25°C and were subjected to a daily dark/light cycle. After two days, rats were randomly separated into five groups and treated with ZnO@Ag@Chitosan NPs and crude metabolites for a month. The final group was given carbendazim 50% WP (Anonymous 2012). The animals were slaughtered after 30 days of therapy, and blood samples were taken to assess the parameters of interest. For the purpose of evaluating toxicological consequences, rats were monitored on a daily basis.

Hematological tests

Blood samples were collected in anticoagulant tubes after 45 days to measure hematological parameters; Red blood cells (RBCs), white blood (WBC) counts and hemoglobin values were determined using the Schalm (1986) method.

Biochemical analysis

After 45 days of recuperation, blood samples were obtained in sterile tubes and centrifuged at 3500 rpm for 20 min to separate the serum. A spectrophotometer set to 400 nm was used to assess the activities of blood serum transaminases such as aspartate transaminase (AST), alanine transaminase (ALT), urea and creatinine. For each sample, five replicates were employed.

Biofungicidal effect of Zno@Ag@chitosan nanoparticles under greenhouses

During the 2020–2021 seasons, the effects of ZnO@Ag@Chitosan NPs as bio fungicides on lowering root rot and wilt disease severity in tomato and cucumber were studied in commercial greenhouses under naturally infected conditions in El Bahera Governorate, Egypt. We employed 500 mg L^{-1} concentrations of ZnO@Ag@Chitosan NPs and crude metabolite. Tomato (*Lycopirsecon esculentum* cv. Bigdena F1) and cucumber (*Cucumis sativus* cv. Rada F1 hybrid) transplanting were coated for 4 h with ZnO@Ag@Chitosan NPs and

surfactant. Control treatments included crude *C. globosum* metabolite at an effective concentration, sterile distilled water, and fungicide (carbendazim 50% WP). During the 2020 and 2021 growing seasons in Giza governorate, experiments were conducted using a randomized full block design with twenty replications. Agricultural practices were followed to the letter.

Disease assay and total yield

During growth periods, the symptoms of illnesses such as root rot, stem cankers and wilt were measured. The total accumulated yield of tomato and cucumber for each treatment was reported at the harvest stage. Twenty plants were taken from each treatment to determine the overall yield per plant (kg plant^{-1}).

The determination of the activities of oxidative enzymes

The effects of ZnO@Ag@Chitosan NPs and crude metabolite treatments on the activities of oxidative defense enzymes, such as peroxidase, polyphenoloxidase and chitinase, in tomato and cucumber plants grown in greenhouses were measured 60 days after transplanting. Leaf samples (g) were homogenized in 0.2 *M* Tris HCl buffer (pH 7.8) containing 14 m*M* mercaptoethanol at a rate of 1/3 w/v at 0°C. A UV spectrophotometer was used to measure the enzyme activities. According to Lee's method, peroxidase activity was measured as an increase in absorbance at 470 nm/g fresh weight/minute (Lee 1973). Polyphenoloxidase activity was measured as an increase in absorbance at 475 nm g^{-1} fresh weight min^{-1} using the Bashan *et al.* (1985) method. Chitinase activity was measured as m*M* N-acetyl glucose amine equivalent released/g fresh weight/60 min at 540 nm (Monreal and Reese 1969).

Estimation of photosynthetic pigments

The amount of photosynthetic pigments, such as chlorophyll a (chl a), chlorophyll b (chl b), and carotenoids, was measured in fresh leaves (mg g 1 of fresh weight) (Königer and Winter1993).

Statistical analysis

Duncan's multiple range test was performed to compare means at P 0.05 levels and ANOVA was utilized to analyze the efficiency of all trials (Duncan 1955). P =0.05 was used as the significant level. The least significant difference (LSD) test was used to compare the means of all five treatments. The STATISTICA-SP statistical software application was used to create similarity coefficients based on pairwise comparisons of treatments based on the existence (1) or absence (0) of unique and shared polymorphism products.

Results

Synthesis and characterization of ZnO@Ag@Chitosan nanoparticles

The biogenesis of ZnO@Ag@Chitosan NPs was studied using UV-visible absorption. The biosynthesis was carried out in two steps: first, the reduction of Ag^+ to atoms in the presence of the *C. globosum* fungus in one pot, then the formation of Zn-OH and subsequently calcination to ZnO in another pot, and finally, the solid-state approach to make ZnO@Ag@Chitosan NPs in a third pot. The density of the yellowish-brown color increases as the surface plasmon resonance of Ag NP is activated. UV-vis spectroscopy in aqueous solution could be used to analyze size-and shape-controlled NPs. The unique absorbance peak in the UV-vis spectrum of ZnO@Ag@Chitosan NPs produced by Fungus was discovered at 430 nm (Fig. 1). Using ATR-FTIR, the stretch vibrations of OH groups were discovered to correspond with the peaks of chitosan at 3431 cm^{-1}. The band at 1635 cm^{-1} has been linked to amide I because proteins have carbonyl extensions. The peak at 1390 cm^{-1} indicates the symmetric deformation vibration mode of CH3, while the peak at 1274 cm^{-1} shows carboxylic acid C-O expansion vibration. The peak of Zn-O of zinc oxide (ZnO) occurs around 490 cm^{-1} in Fig. 2. The zeta potentials of ZnO and Ag@ZnO are -4.85 and 22.27 mV, respectively, as shown in Fig. 2. As illustrated in Fig. 3, the HRTEM was utilized to create ZnO, Ag, and ZnO@Ag@Chitosan NPs.

***In vitro* bioassay**

Agar well diffusion assay: *In vitro* antifungal activity of ZnO@Ag@Chitosan NPs and crude metabolite against *Fusarium oxysporum, Fusarium solani, Sclerotiorum sclerotiorum, R. solani, M. phaseolena, P. parasitica, P. ultimum, A. alternate* and *C. gloeosporioides* is shown in Table 1. The results revealed a distinction between the regimens. ZnO@Ag@Chitosan NPs showed the highest activity when compared to crude metabolite and untreated control. When compared to Carbendazim 50% WP at a concentration of 150 ppm, *R. solani* (33.6 & 34.7 mm) and *F. oxysporum* (30.6 & 35.7 mm) showed the greatest growth inhibition at 250 and 500 mg/l, respectively. ZnO@Ag@Chitosan NPs are also effective against *M. phaseolena* (32.6 & 33.7 mm) and *C. gloeosporioides* at 250 and 500 mg L^{-1} (29.7 & 32.7 mm).

Antioxidant assay of ZnO@Ag@Chitosan NPs by *C. globosum*

Reducing power activity: Activity of ZnO@Ag@Chitosan NPs obtained reducing power which significant increased from (1.5) at 50 mg L^{-1}, (2.8) at 250 mg L^{-1} and to (3.9) at 500 mg L^{-1}concentrations when compared to crude metabolite of *C. globosum* at 500 mg L^{-1} (0.87) (Table 2).

Table 1: Agar well diffusion assay of test plant pathogens with ZnO@Ag@Chitosan NPs and crude metabolite of *C. globosum*

Plant Pathogens	Inhibition (mm)						
	Carbendazim 50% WP	Crude metabolite			ZnO@Ag@Cs NPs		
	(150 ppm)	50 mg L	250 mg L	500 mg L	50 mg L^{-1}	250 mg L	500 mg L
F. oxysporum	36.2 a	05.2 c	10.2bc	22.7a	25.2 a	30.6 c	35.7 a
F. solani	33.2 bc	04.6d	09.5d	20.6c	23.6 b	25.6 e	31.1 bc
S. sclerotiorum	27.2 ef	05.6b	09.6d	20.7c	24.5 ab	28.6 d	32.6 b
R. solani	30.1 d	06.6 a	11.6a	21.6 b	25.6 a	33.6 a	34.7 a
M. phaseolena	31.7 d	06.3 ab	09.4d	21.4 b	24.8 ab	32.6 b	33.7 ab
P. parasitica	34.7 b	05.5bc	09.4d	19.6 cd	23.6 b	29.7 c	31.7 bc
P. ultimum	28.7 e	04.4de	10.4b	18.6 d	22.7 c	27.8 d	29.7 d
A. alternata	25.6 g	04.5d	10.5 b	18.9 d	23.7 b	26.9 de	28.6 d
C. gloeosporioides	30.2 d	05.5bc	10.5b	21.7 b	25.8 a	29.7 c	32.7 b

Values are means of five replications. (c) ANOVA was used to analyses the efficiency of all trials, and Duncan's multiple range test was used to compare means at $P = 0.05$ levels

Table 2: Antioxidant activity of ZnO@Ag@Chitosan nanoparticles produced from *C. globosum*

Antioxidant activity	Crude metabolite			ZnO@Ag@Cs NPs		
	50 (mg L)	250 (mg L)	500 (mg L)	50 (mg L)	250 (mg L)	500 (mg L)
Reducing power assay	0.04 d	0.21 d	0.87 d	1.5 d	2.8 d	3.9 c
DPPH radical scavenging activity (%)	0.05 b	0.67 c	2.20 c	11.0 c	32.8 c	77.5 b
Nitric oxide scavenging assay	0.09 a	0.98 a	32.2 a	71.9 a	86.0 a	89.4 a
ABTS free radical scavenging assay %	0.08 c	0.86 b	13.5 b	36.5 b	55.2 b	75.1 b

Values are means of five replications. (c) ANOVA was used to analyses the efficiency of all trials, and Duncan's multiple range test was used to compare means at $P = 0.05$ levels

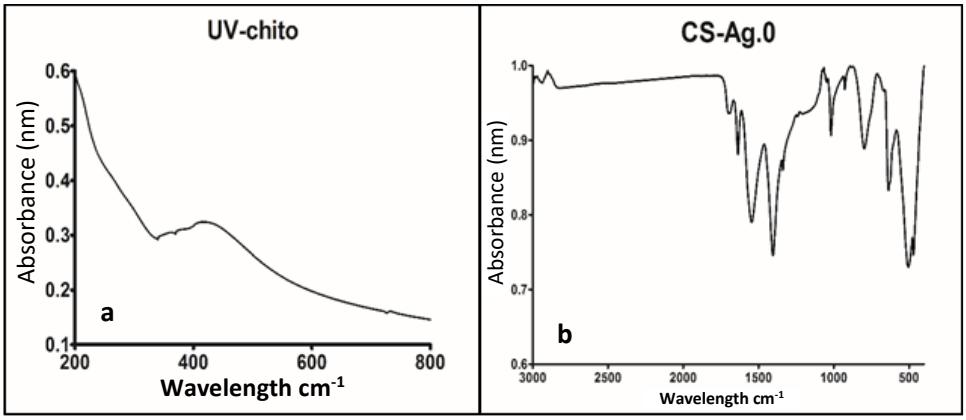

Fig. 1: UV-visible spectra of a) ZnO@Ag@CS and ATR-FTIR b) for *C. globosum*

Diphenyl-1-picryl hydrazyl (DPPH) activity: DPPH radical was utilized to evaluate the scavenging activity of ZnO@Ag@Chitosan NPs. percentage of (11.0) at 50 mg L^{-1} (32.8) at 250 mg L^{-1} and (77.5) at 500 mg $L^{-1}$when compared to crude metabolite of *C. globosum* at 500 mg L^{-1} (2.20) (Table 2).

Nitric oxide scavenging assay: When compared to crude metabolite of *C. globosum*, the ZnO@Ag@Chitosan NPs demonstrated scavenging activity that reach to (71.9) at 50 mg L^{-1} (86.0) at 250 mg L^{-1} and (89.4) at 500 mg L^{-1} when compared to crude metabolite of *C. globosum* at 500 mg L^{-1} (32.2) concentrations (Table 2).

ABTS free radical scavenging activity: ZnO@Ag@Chitosan NPs demonstrated scavenging activity with increasing concentrations, reaching (36.5) at 50 mg L^{-1} (55.2) at 250 mg L^{-1} and (75.1) at 500 mg $L^{-1}$when compared to crude metabolite of *C. globosum* at 500 mg L^{-1} (13.5) (Table 2).

Biosafety and toxicity studies

The most effective concentration (500 mg/L) of both crude extract metabolite and ZnO@Ag@Cs NPs was employed in the bioassay test and antioxidant bioassay.

There is no difference in rats body weight treated with ZnO@Ag@Cs NPs at 500 mG/L (188.9 G) compared to crude metabolite at 500 mg L^{-1} (186.2g) and fungicide, according to Fig. 4. When compared to the untreated control, fungicide produced a decrease in rat body weight (176.7 g) after 45 days (185.0 g). Haemoglobin levels are also significantly lower in rats treated with a chemical fungicide (11.13) compared to ZnO@Ag@Cs NPs (11.84) crude metabolite (11.81) and untreated animals (11.89). The most effective concentration (500 mg L^{-1}) of both crude extract metabolite and ZnO@Ag@Cs NPs was employed in the bioassay test and antioxidant bioassay.

There is no difference in rats body weight treated with

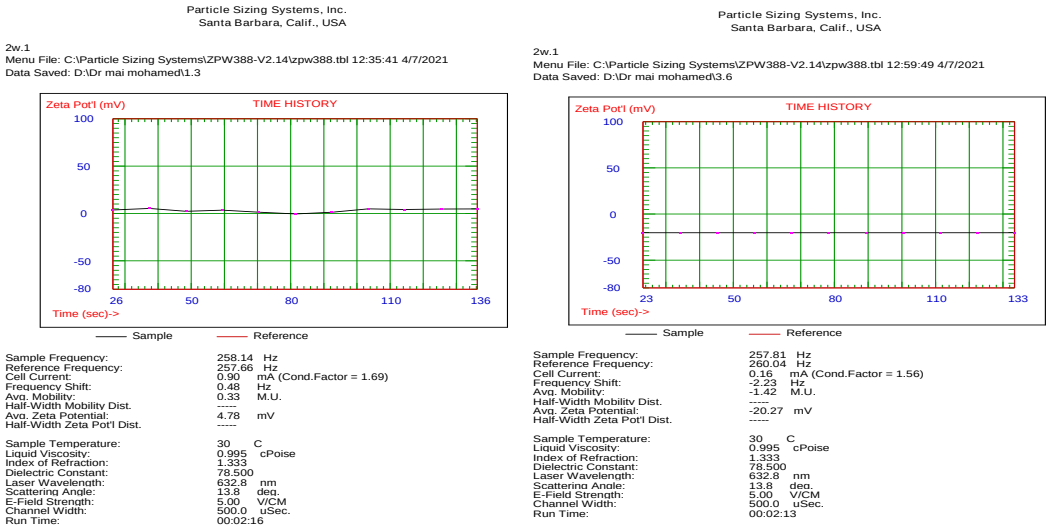

Fig. 2: Zeta potential of ZnO and ZnO@Ag synthesized from *C. globosum*

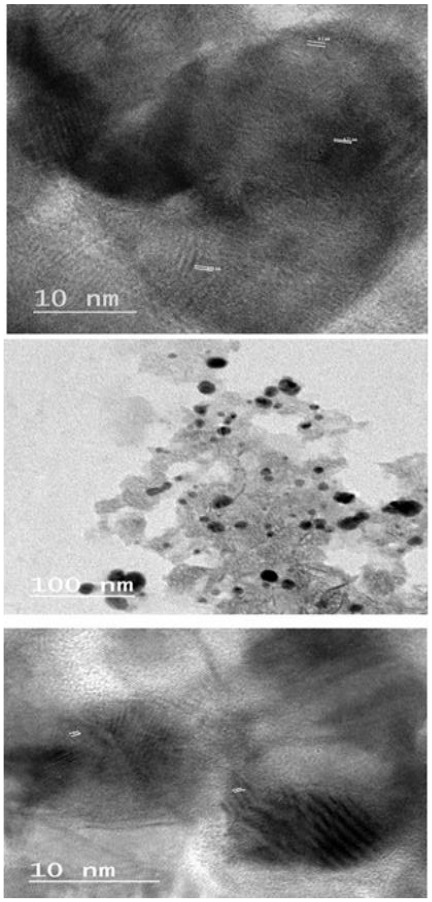

Fig. 3: HRTEM of a) ZnO NPs, b) Ag NPs,c) ZnO@Ag@CS NPs by *C. globosum*

ZnO@Ag@Cs NPs at 500 mg/L (188.9 G) compared to crude metabolite at 500 mg L^{-1} (186.2G) and fungicide, according to Fig. 4. When compared to the untreated control, fungicide produced a decrease in rat body weight (176.7 g) after 45 days (185.0 g). Haemoglobin levels are also significantly lower in rats treated with a chemical fungicide (11.13) compared to ZnO@Ag@Cs NPs (11.84) crude metabolite (11.81) and untreated animals (11.89). When compared to crude metabolites of Chaetomium and ZnO@Ag@Cs NPs, fungicide, and control group (27.5, 28.0, 36.6, and 26.6 mg dL^{-1}, respectively), fungicide significantly increased aspartate transaminase enzyme (AST) activity in treated rats.

There were no significant changes in creatinine concentrations of crude metabolite and ZnO@Ag@Cs NPs (0.90 and 0.89 mg dL^{-1}, respectively) as compared to chemical fungicide (0.93 mg dL^{-1}), which caused a significant increase in creatinine concentration, and untreated control (0.87 mg dL^{-1}). The same results were obtained for urea concentration, with no significant difference between crude metabolite and ZnO@Ag@Cs NPs (33.9 and 33.3 mg dL^{-1}, respectively) and the fungicide (34.8 mg dL^{-1}), which caused a large increase in urea, and the untreated control (31.7 mg dL^{-1}).

Field application

Disease assay: Under natural infection condition of greenhouses, treated tomato and cucumber transplanting with ZnO@Ag@Chitosan NPs biosynthesis from *C. globosum* and its crude metabolite at 500 mg L^{-1} significantly reduced the root-rot, stem canker and wilt diseases in compared with chemical fungicide and untreated control (Table 3). The most effective treatment was ZnO@Ag@Chitosan NPs at 500 mg L^{-1}, which reduced root rot, stem canker, and wilt illnesses by 2.3, 1.0, and 2.7% in tomato plants and 3.0, 0.3 and 2.1% in cucumber plants, respectively, when compared to untreated controls. Tomato plants had 12.7, 9.5 and 25.6% yields, while

Table 3: In greenhouses, potential effect of ZnO@Ag@Chitosan NPs biosynthesis from *C. globosum* and its crude metabolite on root rot and wilt diseases of tomato (A) and cucumber (B) transplanting's

Treatment	Tomato				Cucumber			
	Root rot	Stem cankers	Wilt	Yield (kg Plant^{-1})	Root rot	Stem canker	Wilt	yield (kg Plant^{-1})
Crude metabolite	6.5 ab	3.1 b	6.4 b	6.4 ab	6.6 b	1.8 b	8.8 a	7.7 b
ZnO@Ag@Ch NPs	2.3 d	1.0 c	2.7 d	7.7 a	3.0 c	0.3 d	2.1 c	8.6 a
Fungicide	5.0 bc	1.4 c	5.6 c	5.6 b	4.0 c	0.9 c	3.0 c	6.7 bc
Untreated control	12.7 a	9.5 a	25.6 a	4.6 c	15.0 a	5.6 a	24.7 a	5.1 d

Values are means of twenty replications. (c) ANOVA was used to analyses the efficiency of all trials, and DMR test was used to compare means at $P = 0.05$ levels

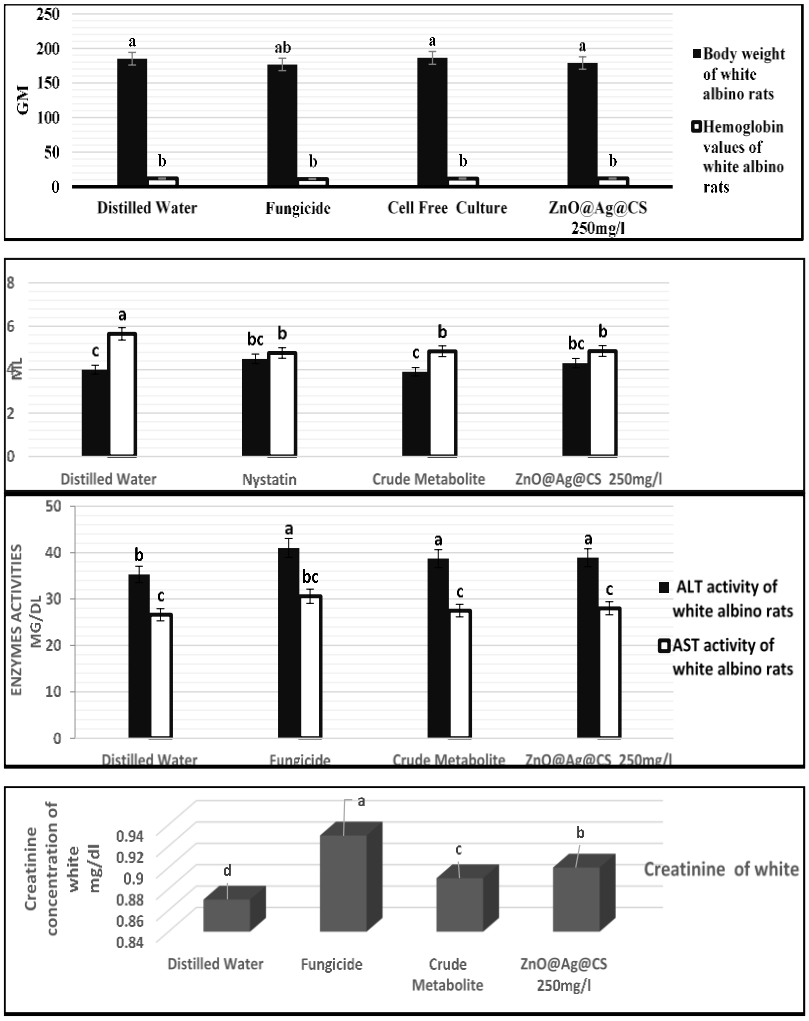

Fig. 4: Histological study, white and red blood cell counts, ALT and AST activities and Creatinine concentrations of white albino treated with ZnO@Ag@Chitosan NPs and crude cell free culture of *C. globosum*. Different letters indicate significant differences among treatments according to the least significant difference test ($P = 0.05$); means of standard deviations for five animals per treatment are shown

cucumber plants had 15.0, 5.6 and 24.7% yields. The disease incidence in treated tomato and cucumber plants was 6.5, 3.1, and 6.4 in tomato and 6.6, 1.8, and 8,8 in cucumber plants, respectively, and the fungicide was 5.0, 1.4 and 5.6 in tomato and 4.0, 0.9 and 3.0 in cucumber. The other treatments were only somewhat successful. Treated plants with ZnO@Ag@Chitosan NPs significant increased yield being (7.7 kg plant^{-1}) of tomato and (8.6 kg plant^{-1}) of cucumber in compared with the crude metabolite at 500 mg L^{-1} by (6.4 and 7.7 kg plant^{-1}) and untreated control (4.6 and 5.1 kg plant^{-1}), respectively (Table 3).

Determination of the activities of oxidative enzymes

The impact of ZnO@Ag@Chitosan NPs at 500 mg L^{-1} treatments on the activities of oxidative defense enzymes such as peroxidase, polyphenoloxidase, and chitinase in tomato and cucumber plants cultivated in greenhouses was

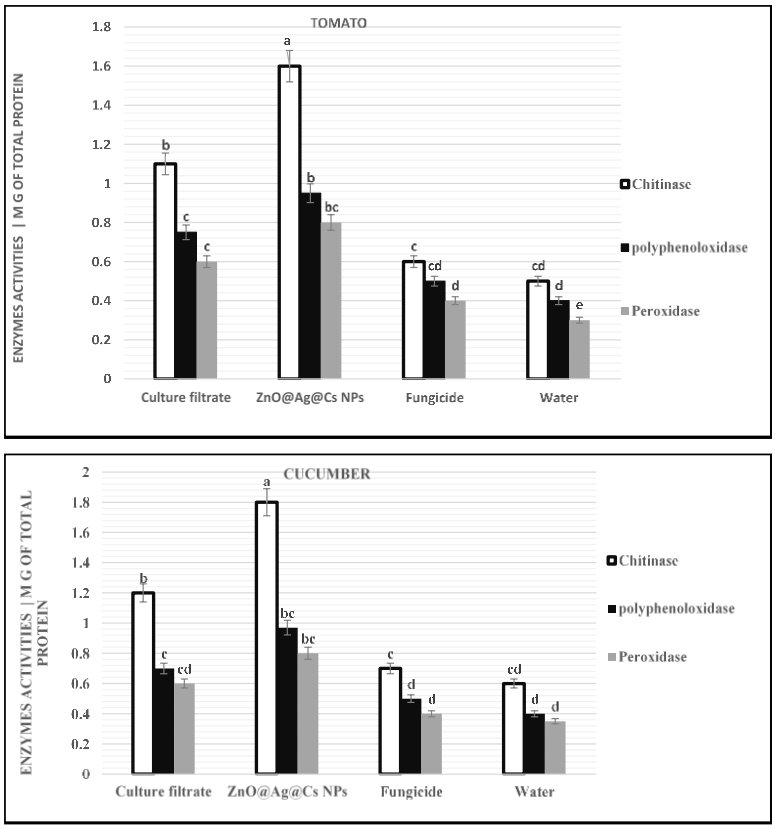

Fig. 5: In greenhouses, potential effect of ZnO@Ag@Chitosan NPs biosynthesis from *C. globosum* and its crude metabolites on oxidative defense enzymes, *i.e*., peroxidase, polyphenoloxidase and chitinase of (A) tomato and (B) cucumber. Different letters indicate significant differences among treatments according to the least significant difference test (P = 0.05); means of standard deviations for twenty plants per treatment are shown

assessed 60 days after transplanting (Fig. 5). When compared to the control and fungicide, the activities of oxidative defense enzymes, such as peroxidase, polyphenoloxidase, and chitinase, were considerably elevated in all treatments of two crops, cucumber and tomato. When cucumber was treated with ZnO@Ag@Chitosan NPs, the activities of peroxidase, polyphenoloxidase and chitinase were 0.8, 0.97, and 1.8, respectively and in tomato, 1.6 mg of total protein, compared to untreated control (0.35, 0.4 and 0.6 mg of total protein) and (0.3, 0.4 and 0.5 mg of total protein). Other treatments recoded moderate activities of all enzymes activities.

Estimated pigment contents

ZnO@Ag@Chitosan NPs at 500 mg/l significantly increased chlorophyll a, b, and carotenoids in tomato and cucumber plants, respectively, with 4.3, 3.9 and 2.7 (FW) (mg g^{-1} FW) for tomato and 4.4, 3.0 and 2.8 (FW) (mg g^{-1} FW) for cucumber, compared to the untreated control. Cucumbers have 3.3, 1.5 and 1.9 (FW) (mg g^{-1} FW), while tomatoes have 3.0, 1.2 and 1.8 (FW) (mg g^{-1} FW) (Fig. 6). The treatment of crude metabolite at 500 mg L^{-1} was relatively effective in raising chlorophyll a, b and c when compared to carotenoids, which were 3.8, 2.0 and 2.1(FW) (mg g^{-1} FW) in tomato and 3.9, 2.9 and 2.4 (FW) (mg g^{-1} FW) in cucumber. The outcomes were less successful in the fungicide and untreated control groups.

Discussion

This study suggested an eco-friendly biofungicide to compact and manage fungal root rot diseases of cucumber and tomato caused by *F. oxysporum*, *F. solani*, *S. sclerotiorum*, *R. solani* and *M. phaseolena.* The finding was confirmed *in vitro* using green biosynthesised ZnO@Ag@Chitosan NPs from *C. globosum*. Green nanotechnology is a novel pesticide alternative that is based on the natural synthesis of nanoparticles from plant and microorganisms (yeast, bacteria, algae, fungi and so on) using environmentally friendly procedures (Karn and Wong 2013; Shah *et al*. 2015).

UV–visible spectroscopy was used to investigate the biosynthesis of ZnO@Ag@Chitosan NPs generated by *C. globosum*. The peak of zinc oxide (ZnO) is around 490 nm. ZnO and Ag@ZnO zeta potentials were found to be -4.85

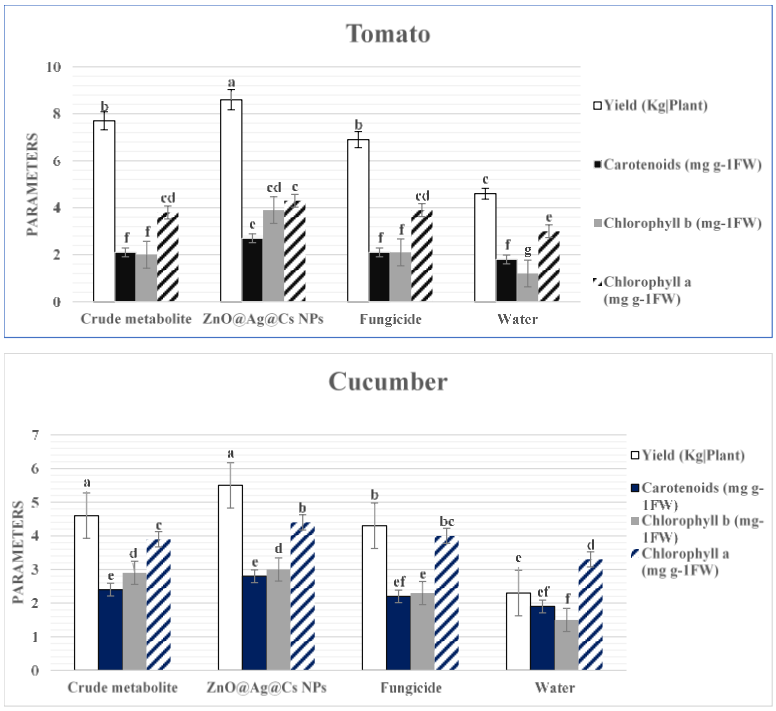

Fig. 6: In greenhouses, potential effect of ZnO@Ag@Chitosan NPs biosynthesis from *C. globosum* and its crude metabolites on chlorophyll a and b and carotenoids of (**A**) tomato and (**B**) cucumber

Different letters indicate significant differences among treatments according to the least significant difference test (P = 0.05); means of standard deviations for twenty plants per treatment are shown

and 22.27 mV, respectively (Samuel *et al*. 2018). The size of spherical nanoparticles in Ag@ZnO@Cs drops considerably due to quantum size confinement and the presence of chitosan in the core-shell (Eid *et al*. 2019).

Due to a wide range of many secondary metabolite contents such as polysaccharides, polyphenols, chitosan, alkaloids, antioxidants, and flavonoids, green nanotechnology has the ability to set bio-nanoparticles (Manikandan *et al*. 2020). The interactions between plants, nanomaterials, microbes, endophytes, and pathogenic fungus have been studied extensively (Farhat *et al.* 2018; Haggag *et al.* 2018; Kalaivani *et al.* 2018; Haggag and Eid 2022). To attain food security, boost crop yield, and reduce pesticide use, Bahrulolum *et al.* (2021) employed microorganisms in the green manufacture of metal nanoparticles.

The antioxidant activity of ZnO@Ag@Chitosan NPs was determined using the reducing power, DPPH, nitric oxide scavenging, and ABTS assays, which are commonly used to investigate the radical scavenging ability of green produced NPs. The antioxidant activity of ZnO@Ag@Chitosan NPs was determined using DPPH, nitric oxide scavenging and the ABTS assay. Biomaterials comprising Ag@Cs NPs and chitosan, according to a prior study, have a high potential for suppressing harmful bacteria (Haggag and Eid 2022).

This suggests that ZnO@Ag@Chitosan NPs have an inhibitory effect on fungal pathogens in plants. The MtNPs' small size and unique physical and chemical properties make them an excellent material in this scenario. Since harmful bacteria are highly inhibited by biomaterials containing ZnO@Ag and chitosan NP.

The potential health benefit of ZnO NPs, which have significant antibacterial and antioxidant activity (Safawo *et al.* 2018), has been a crucial factor. Biopolymer chitosan has a lot of potential in biomedical sectors because of its biocompatibility, biodegradability, non-toxicity, high permeability, antioxidant, and antibacterial characteristics (Kalaivani *et al.* 2018; Hajji *et al.* 2019). Mousa *et al*. (2015), who researched the toxicity of nanopesticide on mice and found it to be less harmful than chemical pesticide, confirm that ZnO@Ag@Cs NPs is a non-toxic pesticide when compared to chemical pesticide. Nanosized silica-silver particles completely controlled powdery mildew disease in cucurbits growing in the field after 21 days of treatment (Park *et al.* 2006). In general, nano fungicides can be utilized to lessen chemical pesticides' environmental and human impacts (Farhat *et al.* 2018; Haggag *et al.* 2018; Haggag and Eid 2022). One of the most often utilized metal oxide nanoparticles is zinc oxide nanoparticles (ZnO-NPs) (Haggag and Eid 2022).

The qualities of NPs, such as size, surface properties and characteristics, solubility, chemical reactivity, physical properties and interactions between nanoparticles and biomolecules *in vivo*, may affect their safety (Bahrulolum *et al*. 2021). The cytotoxicity of NPs was linked to the surface charge of metals, according to Hu *et al.* (2009). The

majority of prior research has found that the cytotoxic and genotoxic effects of Ag NPs are proportional to their size and dosage. Field testing revealed that Chetomium's biosynthesis of ZnO@Ag@Chitosan NPs has biofungicidal capability against soil-borne fungal infections.

The prevention of growth and development was related to the antifungal impact of ZnO@Ag@Chitosan NPs. In addition, when compared to fungicide and control plants, NP application resulted in improved antimycotic effects and plant development. When the chemical fungicide was administered under the same conditions, the outcomes were virtually invariably the same. Farhat *et al.* (2018) discovered that biocontrol agents were more successful in controlling powdery mildew disease and wheat plant growth when they produced silicon and titanium nanoparticles. Chitosan and metal nanoparticles (ZnO@Ag@Chitosan) are more effective at inhibiting the growth of numerous microorganisms than chitosan and metal nanoparticles alone due to their small size, high permeability, biocompatibility, and biodegradability.

As a result, under greenhouse conditions, the ZnO@Ag@Chitosan NPs are likely to be effective in pathogen growth. Similarly, Haggag and Eid (2022) discovered that *Streptomyces aureofaciens* synthesis of Ag@FeO-NPs@Chitosan was effective against several soil-borne fungi, including *F. oxysporum, F. solani, R. solani* and air-borne pathogenic fungi, including *Botrytis cinerea*, *C. gloeosporioides*, *Alternaria solani*, More than 20 pathogenesis genes have been reported to be suppressed by chitosan, including defense enzymes peroxide, polyphenol oxidase, -1,3-glucanase, lignification, chitinase, -gluconase, plant metabolism-related genes, antioxidant, antifungal and antimicrobial (Kalaivani *et al*. 2018; Farhat *et al*. 2018; Hajji *et al*. 2019).

AgNPs were used by Jo *et al*. (2009) to protect tomato plants from fungal pathogens while also increasing plant growth. These *in vivo* studies revealed that the biofungicidal potency of ZnO@Ag@Chitosan NPs could result in the formation of shielding effects of ZnO@Ag@Chitosan NPs around the seedlings' root, acting as a barrier that prevented pathogens from entering the root, colonizing it, and causing disease symptoms. Simultaneously, chitosan can increase the amount of chlorophyll in the body.

Conclusion

Endophytes fungi C. globosum have the potential to be used for the green biosynthesis of ZnO@Ag@Chitosan NPs. The synthesize ZnO@Ag@Chitosan NPs proved antifungal activity against plant pathogens *i.e., R. solani, F. oxysporum, F. solani, S. sclerotiorum, M. phaseolena, P. parasitica, P. ultimum* and have antioxidant activity. White albino haematological aspartate transaminase (AST), alanine transaminase (ALT) and creatinine concentrations demonstrated that ZnO@Ag@Chitosan NPs are safe when compared to fungicide. Furthermore, ZnO@Ag@Chitosan NPs nanoparticles are effective and environmentally friendly as nano-biofungicides in natural greenhouses and can help by reducing root rot, stem canker, and wilt diseases of tomato and cucumber, significantly increasing the activities of oxidative defense enzymes such as peroxidase, polyphenoloxidase and chitinase and photosynthesis concentrations *i.e.*, chlorophyll a, b and carotenoids.

Acknowledgements

This research was funded by the National Research Centre Fund, Egypt, Grant No.12050131 under title: Development and Large-Scale Fermentation Manufacturing of Microbial Biofungicides for Control of some Plant Diseases, from 2019–2022; PI. Wafaa M. Haggag.

Author Contribution

WH and ME planned the experiments and interpreted the results, WH applied of nanoparticles as bio-fungicides and statistically analyzed, and ME prepared and characterize of biosynthesized nanoparticles

Conflict of Interest

The authors declare no conflict of interest.

Data Availability

The reported data can be made available upon requesting to the corresponding author Ethics Approval Not applicable in this research work.

References

Anonymous (2012). *A World Compendium, The Pesticide Manual*, 16th edn. Cohort Software 1986: Costat user's manual virgin 3.03. Berkley, California, USA

Arx JAV, Guarro, MJ Figueras (1986). The Ascomycete Genus Chaetomium. *In: Beihefte zur Nova Hedwigia*, Vol. 84. Lubrecht & Cramer, Berlin, Germany

Bahrulolum H, S Nooraei, N Javanshir, H Tarrahimofrad, VS Mirbagheri, AJ Easton, G Ahmadian (2021). Green synthesis of metal nanoparticles using microorganisms and their application in the agrifood sector. *J Nanobiotechnol* 19:1–26

Bashan Y, Y Okon, Y Henis (1985). Peroxidase, polyphenol oxidase, and phenols in relation to resistance against 214 *Pseudomonas syringae* pv. tomato in tomato plants. *Can J Bot* 65:366–372

Bhardwaj A, D Sharma, N Jodan, P Agrawal (2015). Antimicrobial and phytochemical screening of endophytic fungi isolated from spikes of *Pinus rouxburghii*. *Arch Clin Microbiol* 6:1–9

Duncan DB (1955). Multiple range and multiple F-tests. *Biometrics* 11:1–42

Eid MM, S El-Hallouty, M El-Manawaty, F Abdelzaher (2019). Physicochemical characterization and biocompatibility of SPION@ plasmonic@chitosan core-shell nanocomposite biosynthesized from fungus species. *J Nanomat* 5:1–11

El-Kaed SA, M Mergawy, M Hassanin (2021). Management of the most destructive diseases of chia plant and its impact on the yield. *Egypt J Phytopathol* 49:37–48

Fageria P, S Gangopadhyay, S Pande (2014). Synthesis of ZnO/Au and ZnO/Ag nanoparticles and their photocatalytic application using UV and visible light. *Res Adv* 4:24962–24972

Farhat MG, MH Wafaa, MS Thabet, AA Mosa (2018). Efficacy of silicon and titanium nanoparticles biosynthesis by some antagonistic fungi and bacteria for controlling powdery mildew disease of wheat plants. *Intl J Agric Technol* 14:661–674

Haggag WM, MM Eid (2022). Antifungal and antioxidant activities of Ag@FeONPs@Chitosan preparation by endophyte *Streptomyces aureofaciens*. *Intl J Agric Technol* 18:535–548

Haggag WM, EM Hoballah, R Ali (2018). Applications of nano biotechnological microalgae product for improve wheat productivity in semai aird areas. *Intl J Agric Technol* 14:675–692

Haggag WM, HF Abouziena, F Abd-El-Kreem, SE Habbasha (2015). Agriculture biotechnology for management of multiple biotic and abiotic environmental stress in crops. *J Chem Pharm Res* 7:882–889

Hajji S, SB Khedir, I Hamza-Mnif, M Hamdi, I Jedidi, R Kallel, M Nasri (2019). Biomedical potential of chitosan-silver nanoparticles with special reference to antioxidant, antibacterial, hemolytic and *in vivo* cutaneous wound healing effects. *Biochim Biophys Acta* 1:241–254

Hongtao C, Y Liu, W Ren (2013). Structure switch between α-Fe2O3, γ-Fe_2O_3 and Fe_3O_4 during the large scale and low temperature sol–gel synthesis of nearly monodispersed iron oxide nanoparticles. *Adv Powder Technol* 24:93–97

Hu X, S Cook, P Wang, HM Hwang (2009). *In vitro* evaluation of cytotoxicity of engineered metal oxide nanoparticles. *Sci Total Environ* 407:3070–3072

Hu Y, J Zhang, C Yu, Q Li, F Dong, G Wang, Z Guo (2014). Synthesis, characterization, and antioxidant properties of novel inulin derivatives with amino-pyridine group. *Intl J Biol Macromol* 70:44–49

Javaid A, IH Khan (2016). Management of collar rot disease of chickpea by extracts and soil amendment with dry leaf biomass of *Melia azedarach* L. *Philipp Agric Sci* 99:150–155

Javaid A, S Samad (2012). Screening of allelopathic trees for their antifungal potential against *Alternaria alternata* strains isolated from dying back *Eucalyptus* spp. *Nat Prod Res* 26:1697–1702

Javed S, Z Mahmood, KM Khan, SD Sarker, A Javaid, IH Khan, A Shoaib (2021). Lupeol acetate as a potent antifungal compound against opportunistic human and phytopathogenic mold *Macrophomina phaseolina*. *Sci Rep* 11:1-11

Jo YK, BH Kim, G Jung (2009). Antifungal activity of silver ions and nanoparticles on phytopathogenic fungi. *Plant Dis* 93:1037–1043

Kalaivani R, M Maruthupandy, T Muneeswaran, AH Beevi, M Anand, CM Ramakritinan, AK Kumaraguru (2018). Synthesis of hitosan mediated silver nanoparticles (Ag NPs) for potential antimicrobial applications. *Front LabMed* 2:30–35

Kam B, S Wong (2013). *Sustainable Nanotechnology and the Environment: Advances and Achievements*, pp:1–10. ACS Publications. Washington DC, USA

Khan IH, A Javaid (2022). DNA cleavage of the fungal pathogen and production of antifungal compounds are the possible mechanisms of action of biocontrol agent *Penicillium italicum* against *Macrophomina phaseolina*. *Mycologia* 114:24–34

Khan IH, A Javaid (2020). *In vitro* biocontrol potential of *Trichoderma pseudokoningii* against *Macrophomina phaseolina*. *Intl J Agric Biol* 24:730–736

Köniğer M, K Winter (1993). Reduction of photosynthesis in sun leaves of *Gossypium hirsutum* L. under conditions of highlight intensities and suboptimal leaf temperatures. *Plant Physiol* 13:659–668

Kutawa AB, K Ahmad, A Ali, MZ Hussein, MAA Wahab, A Adamu, AA Ismaila, MT Gunasena, MZ Rahman, MI Hossain (2021). Trends in nanotechnology and its potentialities to control plant pathogenic fungi: A review. *Biology* 10:1–26

Lee T (1973). On extraction and quantitation of plant peroxidase isoenzymes. *Physiol Plant* 29:198–203

Lu CH, CC Lan, YL Lai, YL Li, CP Liu (2011). Enhancement of green emission from InGaN/GaN multiple quantum wells *via* coupling to surface plasmons in a two-dimensional silver array. *Adv Funct Mater* 21:4719–4723

Manikandan R, R Kavitha, W Pan, M Elanchezhian, S Selvakumar (2020). Biogenic synthesis of nanoparticles and their environmental applications. *In: Biological Synthesis of Nanoparticles and Their Applications* Vol. 2, 8th edn, p:298. CRC Press, New York, USA

Marcocci L, JJ Maguire, M Droy-Lefaix, L Packer (1994). The nitric oxide-scavenging properties of Ginkgo biloba extract EGb 761. *Biochem Biophys Res Commun* 15:748–755

Monreal J, T Reese (1969). The chitinase of *Serratia marcescens*. *Can J Microbiol* 15:689–696

Mousa AA, A Hassan, R Mahindra, S Ernest, A Kamel (2015). Myconanoparticles: Synthesis and their role in phytopathogens management. *Biotechnol Equip* 29:221–236

Moya P, D Pedemonte, S Amengual, MEE Franco, MN Sisterna (2016). Antagonism and modes of action of *Chaetomium globosum* species group, potential biocontrol agent of barley foliar diseases. *Bol Soc Argent Bot* 51:569–578

Okamoto K, K Tateishi, K Tamada, M Funato, Y Kamakami (2019a). Micro-photoluminescence mapping of surface plasmon-coupled emission from InGaN/GaN quantum wells. *Jap J Appl Phys* 58:31–35

Okamoto K, K Tateishi, K Tamada, M Funato, Y Kawakami (2019b). Micro-photoluminescence mapping of surface plasmon-coupled emission from InGaN/GaN quantum wells Koichi. *Jap J Appl Phys* 58:1–5

Osman M, MM Eid, OH Khattab, SM El-Hallouty, DA Mahmoud (2016). Biosynthesis of silver nano-particless by local fungal isolates from Egyptian soil. *Quant Mat* 5:305–311

Oyaizu M (1986). Studies on products on browning reaction prepared from glucose amine. *Jap J Nutr* 44:307–315

Park HJ, SH Kim, HJ Kim, SH Choi (2006). A new composition of nanosized silica-silver for control of various plant diseases. *Plant Pathol J* 22:295–302

Safawo T, BV Sandeep, S Pola, A Tadesse (2018). Synthesis and characterization of zinc oxide nanoparticles using tuber extract of anchote (*Coccinia abyssinica* (Lam.) Cong.) for antimicrobial and antioxidant activity assessment. *Open Nano* 3:56–63

Samuel MS, V Subramaniyan, J Bhattacharya, C Parthiban, S Chand NP Singh (2018). A GO-CS@ MOF [Zn (BDC)(DMF)] material for the adsorption of chromium (VI) ions from aqueous solution. *Compos B Eng* 152:116–125

Schalm OW (1986). *Veterinary Hematology*, 4th edn, pp:21–86. Loa and Fibiger, Philadelphia

Shah M, D Fawcett, S Sharma, SK Tripathy, GEJ Poinern (2015). Green synthesis of metallic nanoparticles *via* biological entities. *Materials* 8:7278–7308

Sharf W, A Javaid, A Shoaib, IH Khan (2021). Induction of resistance in chili against *Sclerotium rolfsii* by plant growth promoting rhizobacteria and *Anagallis arvensis*. *Egypt J Biol Pest Contr* 31:16

Um-e-Aiman N, T Tsuzuki, A Lowe, JT Rossiter, A Javaid, G Powell, R Waseem, SH Al-Mijalli, M Iqbal (2021). Chitin nanofibers trigger membrane bound defence signalling and induce elicitor activity in plants. *Intl J Biol Macromol* 178:253–262

Vijayakumar ST, S Karthikeyeni, S Vasanth, A Ganesh, G Bupesh, R Ramesh, M Manimegalai, P Subramanian (2013). Synthesis of silver-doped zinc oxide nanocomposite by pulse mode ultrasonication and its characterization studies. *J Nanosci* 2013:785064

Wang JX, X Sun, Y Yang, H Huang, YC Lee, O Tan, L Vayssieres (2006). Hydrothermally grown oriented ZnO nanorod arrays for gas sensing applications. *Nanotechnology* 17:4995–4998

Yang P, H Yan, S Mao, R Russo (2002). Controlled growth of ZnO nanowires and their optical properties. *Adv Funct Mat* 12:323–331

Zhang R, P Yin, N Wang, L Guo (2009). Photoluminescence and raman scattering of ZnO nanorods. *Solid State Sci* 11:865–869

Zheng Y, LY Zheng, Y Zhan, X Lin, Q Zheng, K Wei (2007). Ag/ZnO heterostructure nanocrystals: Synthesis, characterization, and photocatalysis. *Inorg Chem* 46:6980–6986

Zhishen J, T Mengcheng, W Jianming (1999). The determination of flavonoid contents in mulberry and their scavenging effects on superoxide radicals. *Food Chem* 64:555–559

Zhou XD, XH Xiao, JX Xu, GX Cai, F Ren, CZ Jiang (2011). Mechanism of the enhancement and quenching of ZnO photoluminescence by ZnO-Ag coupling. *Europhys Lett* 93:57009